



Originally published as:

Crowley, G., Knipp, D. J., Drake, K. A., Lei, J., Sutton, E., Lühr, H. (2010): Thermospheric density enhancements in the dayside cusp region during strong BY conditions. - Geophysical Research Letters, 37, L07110

DOI: [10.1029/2009GL042143](https://doi.org/10.1029/2009GL042143)



Thermospheric density enhancements in the dayside cusp region during strong B_Y conditions

G. Crowley,^{1,2} D. J. Knipp,³ K. A. Drake,⁴ J. Lei,⁵ E. Sutton,⁶ and H. Lühr⁷

Received 28 December 2009; revised 15 February 2010; accepted 23 February 2010; published 14 April 2010.

[1] Tri-axial accelerometer data from the Challenging Minisatellite Payload (CHAMP) satellite have revealed the thermospheric density and its variability in unprecedented detail. The data often contain regions of high density located in the cusp sector at high latitudes. In this paper we provide the first detailed explanation of a high latitude density enhancement observed by CHAMP, focusing on the August 24, 2005 interval. The Thermosphere Ionosphere Mesosphere Electrodynamics General Circulation Model (TIMEGCM) was driven by high-fidelity high-latitude inputs specified by the Assimilative Mapping of Ionospheric Electrodynamics (AMIE) algorithm, and reproduced the main features of the density enhancements. The TIMEGCM and AMIE provide a global framework for interpretation of the CHAMP densities. Our simulations reveal that the observed density enhancement in the dayside cusp region resulted from unexpectedly large amounts of energy entering the Ionosphere-Thermosphere system at cusp latitudes during an interval of strong (+20 nT) B_Y . **Citation:** Crowley, G., D. J. Knipp, K. A. Drake, J. Lei, E. Sutton, and H. Lühr (2010), Thermospheric density enhancements in the dayside cusp region during strong B_Y conditions, *Geophys. Res. Lett.*, 37, L07110, doi:10.1029/2009GL042143.

1. Introduction and Background

[2] As more objects have been placed into orbit in the thermosphere it has become more important to understand the density variability because variable satellite drag adversely affects spacecraft missions. In the present era, the Challenging Minisatellite Payload (CHAMP) satellite and its sensitive tri-axial accelerometer [Bruinsma and Biancale, 2003; Liu *et al.*, 2005] have revealed the density variability in unprecedented detail. The satellite provides near-global latitudinal coverage at ~400 km altitude in all local time sectors. Lühr *et al.* [2004] showed that the CHAMP data often contain regions of high density located in the noon sector at high latitudes correlated with the location of small-scale field-aligned currents associated with the dayside cusp. These density features were often observed under relatively quiet geomagnetic condi-

tions. The heating near the dayside cusp in quiet times was not thought to be particularly large, and its ability to produce density enhancements was expected to be limited. Therefore the CHAMP enhancements were a mystery. Liu *et al.* [2010] provide a survey of mass density enhancements in the polar cap during magnetic storms with $D_{ST} < -100$ nT between 2002–2005).

[3] Initially it was thought that the density enhancements might be a manifestation of the organized density structures in the high latitude neutral thermosphere found by Crowley *et al.* [1989], consisting of pairs of high- and low-density regions with diameters of 1000 to 2000 km. These density ‘cells’ were first found in simulations of storm intervals using the NCAR TGCM. Later, evidence for the predicted cellular structure was found in satellite data from the S85-1 and other satellites [e.g., Crowley *et al.*, 1996]. The mechanisms for the cell formation were discussed by Schoendorf *et al.* [1996] and by R. L. Walterscheid and G. Crowley (High latitude thermal cells induced by ion drag driven gyres, manuscript in preparation, 2010). They are a result of the pressure gradient required to balance the centripetal and Coriolis forces that arise from winds in the cyclonic and anticyclonic vortices. The density in each ‘cell’ is enhanced or depleted from the hemispheric average by up to 30% during magnetically active times (with large wind speeds), and the density perturbations are particularly large in the 160–300 km region. However, the large density enhancements observed by CHAMP [Lühr *et al.*, 2004] occurred at altitudes above 300 km during relatively quiet conditions, which did not fit this “density cell” model. Schlegel *et al.* [2005] attempted to simulate one of the density enhancements reported in Lühr *et al.* for a quiet day using the TIMEGCM, but the model was unable to reproduce the observations. The possible reason will be discussed later.

[4] This paper provides the first detailed explanation of a high latitude density enhancement observed by CHAMP. The TIME-GCM model was driven by high-fidelity high-latitude inputs specified by the Assimilative Mapping of Ionospheric Electrodynamics (AMIE) algorithm, and reproduces the CHAMP density enhancements.

2. Model Description

[5] The TIME-GCM is the latest in a series of 3-D models developed at NCAR that includes the stratosphere, mesosphere and thermosphere [Roble and Ridley, 1994]. The model is resident at ASTRA and has been used extensively in studies of the dynamics of the MLT [Meier *et al.*, 2005; Schlegel *et al.*, 2005; Crowley and Meier, 2008; Walterscheid and Crowley, manuscript in preparation, 2010]. In this paper, the TIME-GCM was driven by high latitude inputs from the AMIE algorithm that ingests data from a wide range of sources to produce a realistic representation of the high

¹ASTRA, San Antonio, Texas, USA.

²Department of Physics and Astronomy, UTSA, San Antonio, Texas, USA.

³High Altitude Observatory, NCAR, Boulder, Colorado, USA.

⁴CIRES, University of Colorado at Boulder, Boulder, Colorado, USA.

⁵Aerospace Engineering Sciences Department, University of Colorado at Boulder, Boulder, Colorado, USA.

⁶AFRL, Hanscom Air Force Base, Massachusetts, USA.

⁷Deutsches GeoForschungsZentrum, Potsdam, Germany.

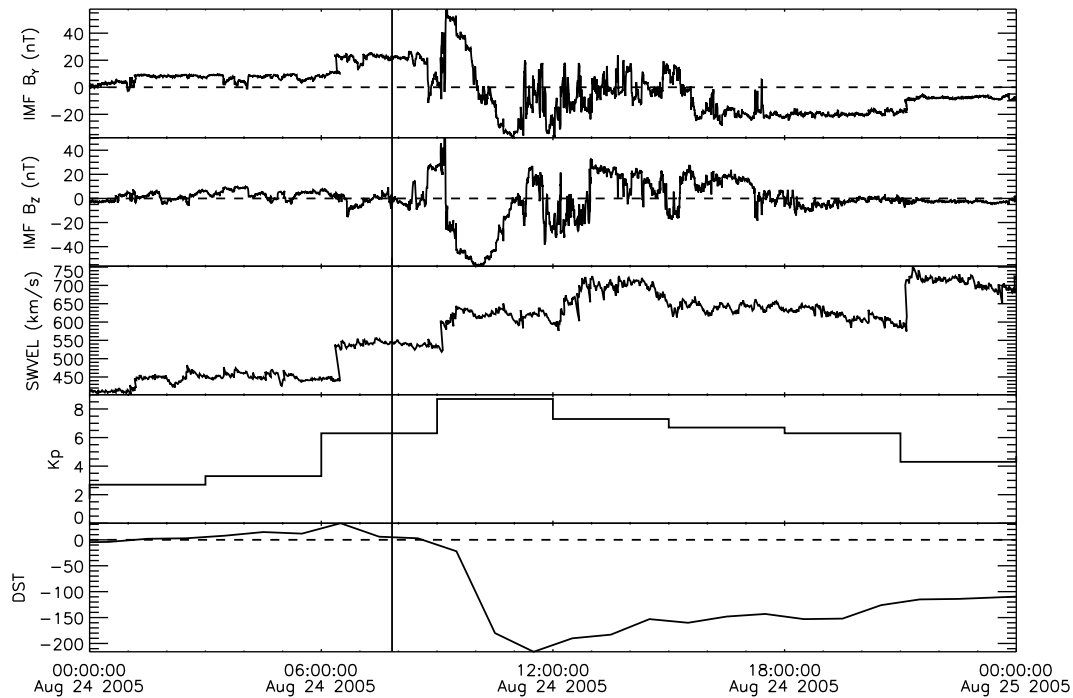


Figure 1. IMF parameters and K_p and D_{ST} indices for August 24, 2005.

latitude electrodynamic state [Richmond and Kamide, 1988]. For this study, the data inputs included electric fields derived from 200 magnetometers, three DMSP satellites, and 11 SuperDARN radars.

3. Results

[6] Figure 1 shows the solar wind and Interplanetary Magnetic Field (IMF) parameters during August 24, 2005. Beginning at ~ 06 UT on August 24, a solar wind shock arrived at the magnetopause ushering in an interval of strongly positive B_Y . B_Y remained near +20 nT for almost three hours, while B_Z fluctuated between +10 nT and -10 nT. A vertical line is shown at 0750, which is close to when DMSP passed through the cusp region, as discussed below. For several hours afterwards both B_Z and B_Y contained strong fluctuations, until about 1545UT, when B_Y turned strongly negative (-20 nT) and remained negative through the end of the day. The bottom panels of Figure 1 show the K_p and D_{ST} indices, which will be discussed below.

[7] Figure 2 shows CHAMP densities (black line) as a function of Universal Time (UT) for three orbits on August 24, 2005. The dataset used in this study consists of total mass densities processed by the Space Physics and Aeronomy group at the University of Colorado at Boulder, Version 2.2 [Sutton *et al.* 2007]. Figure 2 (bottom) depicts the corresponding latitude and local time of the spacecraft. The density characteristics of the orbit beginning about 06:50 UT are quite different from the previous orbits. In particular, there are large enhancements in the southern polar region near 07:00 UT, and in the northern hemisphere near 07:35 UT. Superposed on Figure 2 are predictions from the TIME-GCM that reproduce the observed density enhancements reasonably well.

[8] D. J. Knipp *et al.* (Extreme Poynting flux delivered to the thermosphere during intervals of large east-west inter-

planetary magnetic field, manuscript in preparation, 2010) found that during the event considered here and at other times of solar wind shocks with strongly northward B_Z or strong B_Y conditions reconnection tends to occur on the magnetotail lobes, significant energy is delivered to high latitude, dayside regions without evidence of strong night-side convection or substorm. As a result, the ring current does not grow, and therefore the D_{ST} index shows little response to these events (see Figure 1). Thus, thermospheric density models based on the D_{ST} index are unable to predict the observed density enhancements. Knipp *et al.* (manuscript in preparation, 2010) looked at data from the Defense Meteorological Satellite Program (DMSP) F15 satellite during times in which the CHAMP satellite saw density enhancements that were not predicted by such thermospheric density models. Specifically, they found unexpected localized enhancements in the Poynting flux in the near-cusp region.

[9] While the CHAMP density enhancement was observed about 07:30 UT, the closest DMSP F15 pass was a few minutes later at 07:38–07:58 UT (Figure 3a), with strong localized Poynting flux in the cusp region near noon and 70° magnetic latitude, as described in detail by Knipp *et al.* (manuscript in preparation, 2010). DMSP passed through the cusp Poynting flux enhancement about 07:50 UT, and Figures 3b–3d depict the corresponding electrodynamic parameters for 07:50 UT from AMIE, with the DMSP F15 location superposed. (Note that the AMIE patterns were available every 5 min, and maintained an essentially similar pattern from 06:30–8:30 UT, so the exact time chosen here is unimportant. The pattern had already set up a density enhancement in the southern hemisphere by 07:00 UT that was observed by CHAMP, as seen in Figure 2). The potential pattern is shown in Figure 3b and consists of two cells, with the larger cell occurring in the afternoon sector, typical of strong B_Y positive conditions. The same DMSP pass is shown

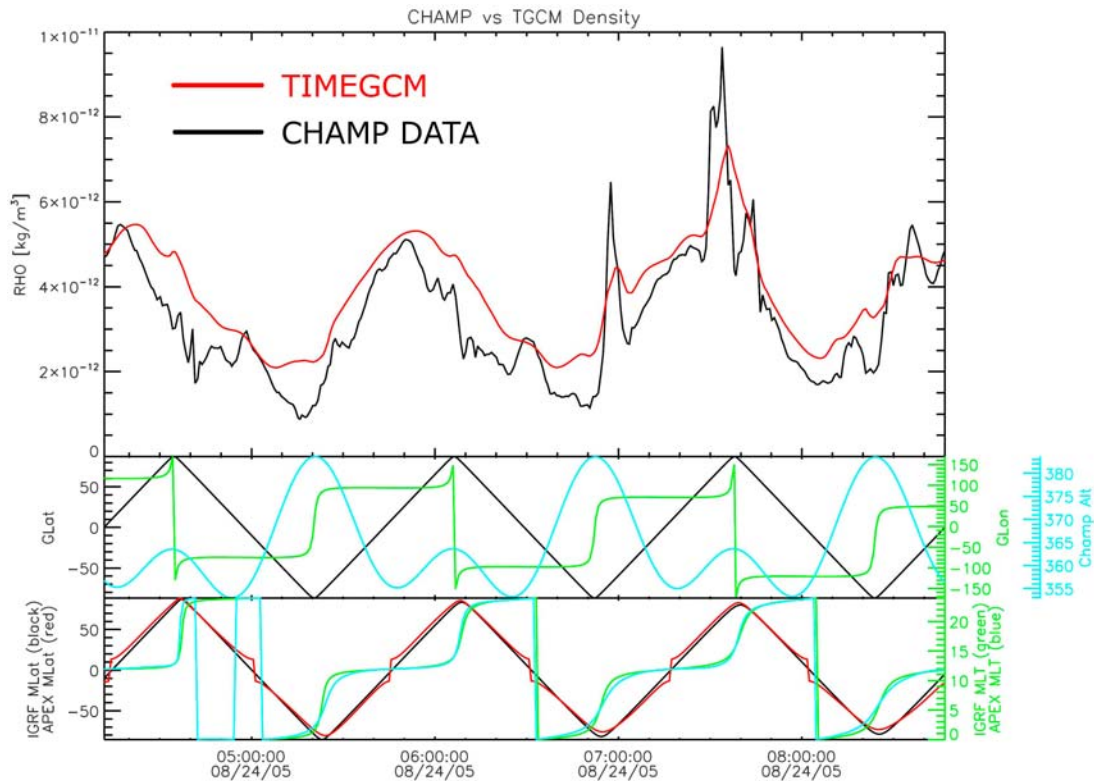


Figure 2. (top) Line plot showing densities measured (black line) during three orbits of the CHAMP satellite as a function of UT on August 24, 2005. TIME-GCM predicted densities (red line) are superposed. (middle) Geographic latitude, longitude and altitude of CHAMP. (bottom) Geomagnetic (Apex and IGRF) latitude and longitude of CHAMP.

in Figure 3b measurements. The convection pattern reveals strong electric fields near the location where DMSP observed large Poynting fluxes. Figures 3c and 3d illustrate the corresponding Joule heating and downward Field Aligned Currents (FAC) obtained for this time. The maximum Joule heating occurs along the DMSP track at the same location as the enhanced Poynting Flux (PF). A comparison of the magnitudes of the Joule heating (Figure 3c) and Poynting flux (Figure 3a) reveals that the maximum PF value is 150 mW/m^2 , whereas the maximum Joule heating value is 60 mW/m^2 . The reason for this discrepancy is mainly that the resolution of AMIE is too coarse to capture the details observed by DMSP, and the DMSP data were smoothed prior to assimilation by AMIE. However, the global AMIE patterns confirm that the energy deposition region is truly limited to the noon sector, as suggested by the DMSP measurements. The strong field-aligned currents evident in the AMIE output produced the δB measured by DMSP and used in the Poynting flux calculation. The region of strong field-aligned currents is also limited to the noon sector.

[10] The AMIE fields were obtained with a cadence of 5 minutes and used to drive the TIME-GCM, which used a model time-step of 30 seconds. Figure 4 shows the TIME-GCM mass density at 400 km for the northern hemisphere at 07:35 UT. The locations of the CHAMP satellite for 10 minutes centered at 07:35 UT are superposed on Figure 4, revealing that CHAMP was passing through an isolated density enhancement near the pole at that time. This is the same feature that was responsible for the density spike

observed by CHAMP (see Figure 1) at 07:35 UT near the North Pole.

4. Discussion

[11] AMIE convection and precipitation patterns were used to specify the high latitude inputs for the TIMEGCM during the 24 August 2005 interval, resulting in an isolated large density enhancement in the cusp region, similar to that observed by CHAMP. Although the TIME-GCM was used by Schlegel *et al.* [2005] to simulate density structures, their simulation failed to reproduce the density enhancements observed by CHAMP. We suggest the reason may be that AMIE was not used as the high latitude driver, but the much simpler Heelis *et al.* [1982] convection model. The Heelis model utilizes a two-cell convection pattern with limited ability to rotate under the influence of B_Y . It would be unable to produce a convection pattern like the AMIE convection pattern shown in Figure 3.

[12] The key data input in the present AMIE runs was the DMSP data. When only magnetometers were ingested, The corresponding potential patterns were much smoother and the cross-cap potential was underestimated (Y. Deng, private communication, 2009), and a thermospheric model driven by such AMIE patterns was unable to reproduce the Joule heating peak in the noon sector, and as a result failed to produce the observed density enhancement.

[13] In addition to the auroral electron inputs as specified by AMIE, precipitating ions can represent a significant

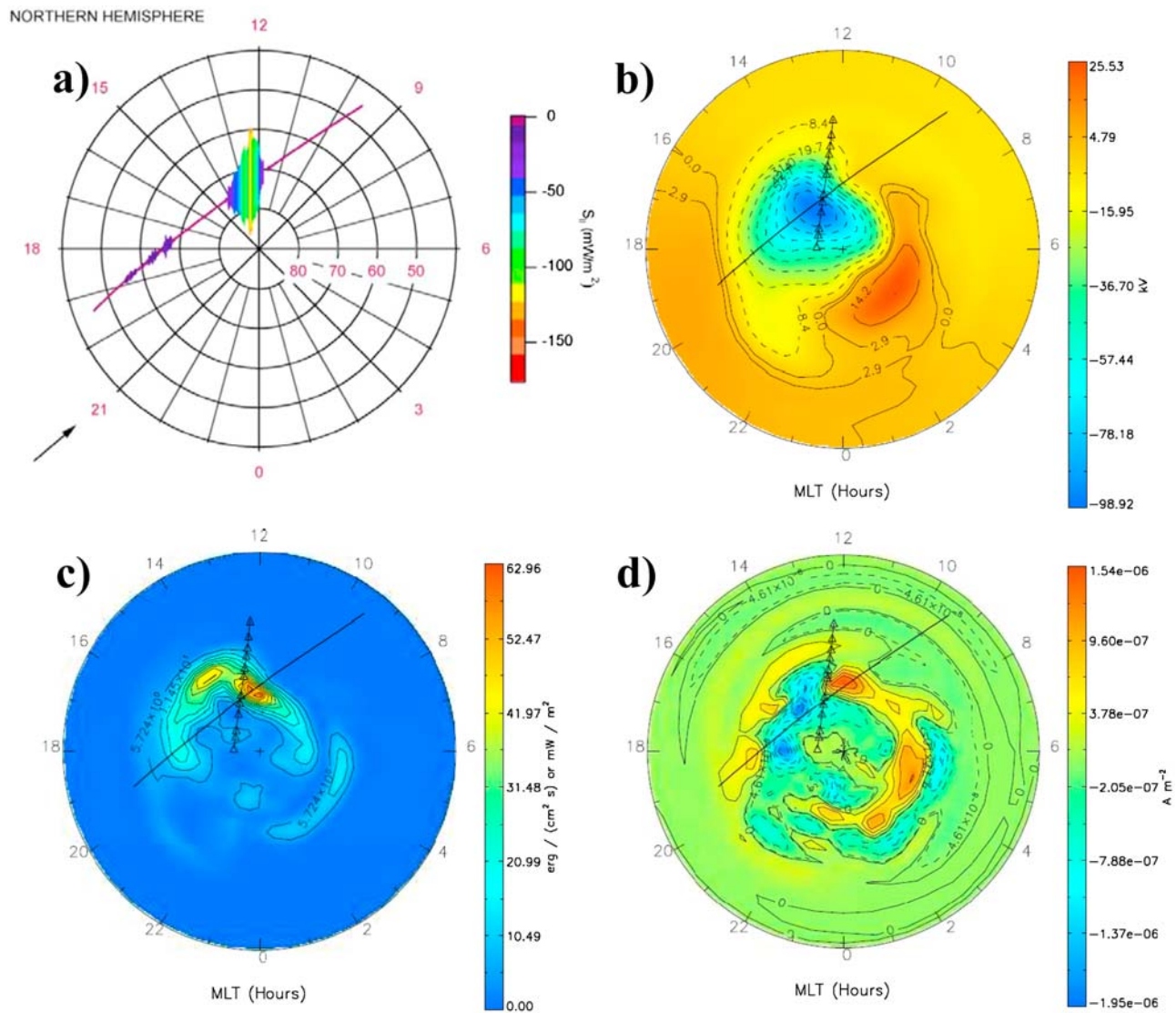


Figure 3. Electrodynamic quantities for 07:50 UT. (a) DMSP track from 07:38–07:58 UT with Poynting flux superposed, after Knipp et al. (manuscript in preparation, 2010). (b) AMIE convection pattern with locations of DMSP from 07:38–07:58 UT (solid curve) and CHAMP from 07:30–07:39 UT (symbols). (c) Height-integrated Joule heating distribution from AMIE. (d) Downward field-aligned currents from AMIE. In Figures 3b–3d, DMSP. Outer latitude is 40° magnetic latitude.

energy source to the atmosphere that was not included here. Significant changes in the conductance (and thus Joule heating) can be caused by proton precipitation [e.g., Fang et al., 2007], and significant heating by oxygen ion precipitation [e.g., Ishimoto et al., 1992] that might also be contributing to the observed event, but this is beyond the scope of the current study.

[14] This paper has focused on the dayside density enhancements for a single event during an interval of strong B_Y positive. However, we have examined the entire August 24–25 period, and found similar enhancements in the cusp-region Poynting flux, and Joule heating between about 15:45–23:00 UT on August 24, during times when the IMF B_Y was strongly negative. The isolated heating near the pole resulted in another density enhancement that was observed by CHAMP over several consecutive orbits. This later period will be the topic of another, more extended, paper.

[15] The intervening period between about 09:00 UT and 15:45 UT was a period of strong negative B_Z . During this time, the K_P index jumped to 9. Therefore the interval cannot be classified as quiet. Figure 1 depicted the K_P index along with the IMF conditions, and showed that even the interval between 06–09 UT was at moderately active K_P levels ($K_P = 6$), even though D_{ST} did not go negative until 8.30 UT. Lühr et al. [2004] found that many of their CHAMP density enhancements occurred during quieter conditions, and it will require more work to determine whether those quiet-time events were likewise caused by high latitude (cusp) heating from strong northward B_Z or B_Y conditions.

[16] Finally, we have also examined the wind patterns (not shown) during the density enhancements reported here, to determine whether these events could have been formed by the fluid-dynamical mechanisms associated with the Crowley “cells”. The high density region is not consistent with the

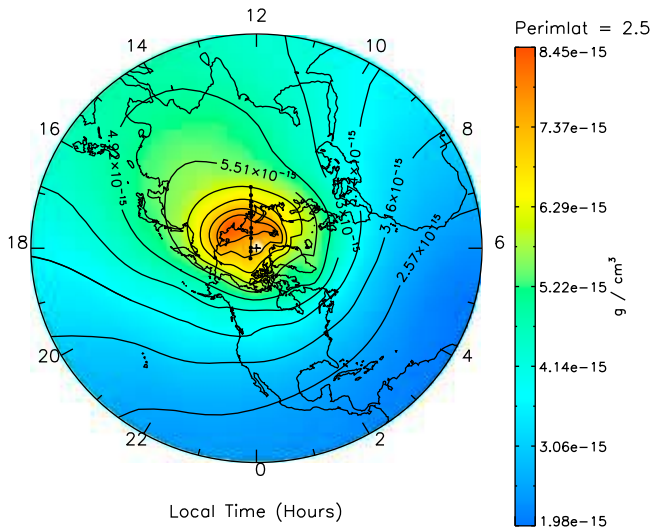


Figure 4. Neutral density distribution from TIME-GCM for 07:35 UT. Black dots indicate CHAMP locations from 7:30–7:39 UT. Outer latitude 2.5 degrees geographic latitude.

winds required by the ‘cell’ mechanism, but rather appears to be forced by direct Joule heating.

[17] Empirical models such as *Jacchia* [1970] or MSIS-00 [Picone et al., 2002] are smooth at high latitudes because they lack the data to justify higher harmonics in their basis functions. They also are unable to respond to events such as the one presented here, due to having inappropriate drivers. If operational models are to accurately represent density enhancements such as the ones studied here, it seems likely they will need to be first principles models driven by realistic, high fidelity, convection patterns such as those from AMIE with multiple data sets being assimilated.

[18] **Acknowledgments.** G.C. was supported at UTSA by AFOSR MURI award FA9550-07-1-0565, and at ASTRA by NSF GEM award ATM-0703335 and NASA awards NNX07AB66G and NNG04GN04G. D.J.K. was supported in part by AFOSR contract FA9550-08-C-0046. K.A.D. was supported by AFSOR grant FA7000-08-D-0025/26. We are grateful to the following data providers: the Center for Space Sciences at the University of Texas at Dallas provided DMSP SSIES data; SuperDARN data was provided by J. M. Ruohoniemi and the Johns Hopkins University APL; Magnetometer data were provided by: the Solar-Terrestrial Environment Laboratory, Nagoya University; the World Data Centre (WDC) for Solar-Terrestrial Science (STS) operated by IPS Radio and Space Services, Australia; the Canadian Space Science Data Portal and the University of Alberta; the Geophysical Institute of the University of Alaska and PURAES (Project for Upgrading Russian AE Stations); Danish Meteorological Institute and Space Physics Research Laboratory at the University of Michigan; INTERMAGNET; Eftyhia Zesta; Space Plasma Environment and Radio Science (SPEARS) in the Department of Communication Systems at the Lancaster University; Institute for Physical Science and Technology at the University of Maryland; WDC for Geomagnetism, Edinburgh. Satellite magnetometer data were provided by the AF Research Laboratory.

References

Bruinsma, S., and R. Biancale (2003), Total densities derived from accelerometer data, *J. Spacecr. Rockets*, *40*, 230–236, doi:10.2514/2.3937.

- Crowley, G., and R. R. Meier (2008), Disturbed O/N₂ ratios and their transport to middle and low latitudes, in *Midlatitude Ionospheric Dynamics and Disturbances*, *Geophys. Monogr. Ser.*, vol. 181, edited by P. M. Kintner Jr. et al., pp. 221–234, AGU, Washington, D. C.
- Crowley, G., B. A. Emery, R. G. Roble, H. C. Carlson, and D. J. Knipp (1989), Thermospheric dynamics during September 18–19, 1984: 1. Model simulations, *J. Geophys. Res.*, *94*, 16,925–16,944, doi:10.1029/JA094iA12p16925.
- Crowley, G., J. Schoendorf, R. G. Roble, and F. A. Marcos (1996), Cellular structures in the high-latitude thermosphere, *J. Geophys. Res.*, *101*, 211–223, doi:10.1029/95JA02584.
- Fang, X., M. W. Liemohn, J. U. Kozyra, and D. S. Evans (2007), Global 30–240 keV proton precipitation in the 17–18 April 2002 geomagnetic storms: 2. Conductances and beam spreading, *J. Geophys. Res.*, *112*, A05302, doi:10.1029/2006JA012113.
- Heelis, R., J. Lowell, and R. Spiro (1982), A model of the high-latitude ionospheric convection pattern, *J. Geophys. Res.*, *87*, 6339–6345, doi:10.1029/JA087iA08p06339.
- Ishimoto, M., G. J. Romich, and C. I. Meng (1992), Energy distribution of energetic O⁺ precipitation into the atmosphere, *J. Geophys. Res.*, *97*, 8619–8629, doi:10.1029/92JA00228.
- Jacchia, L. G. (1970), New static models of the thermosphere and exosphere with empirical temperature profiles, *Smithson. Astrophys. Spec. Rep.*, 313.
- Liu, H., H. Lühr, V. Henize, and W. Köhler (2005), Global distribution of the thermospheric total mass density derived from CHAMP, *J. Geophys. Res.*, *110*, A04301, doi:10.1029/2004JA010741.
- Liu, R., H. Lühr, and S.-Y. Ma (2010), Storm-time related mass density anomalies in the polar cap as observed by CHAMP, *Ann. Geophys.*, *28*, 165–180.
- Lühr, H., M. Rother, W. Köhler, P. Ritter, and L. Grunwaldt (2004), Thermospheric up-welling in the cusp region, evidence from CHAMP observations, *Geophys. Res. Lett.*, *31*, L06805, doi:10.1029/2003GL019314.
- Meier, R. R., G. Crowley, D. J. Strickland, A. B. Christensen, L. J. Paxton, and D. Morrison (2005), First look at the 20 November 2003 superstorm with TIMED/GUVI: Comparisons with a thermospheric global circulation model, *J. Geophys. Res.*, *110*, A09S41, doi:10.1029/2004JA010990.
- Picone, J. M., A. E. Hedin, D. P. Drob, and A. C. Aikin (2002), NRLMSISE-00 empirical model of the atmosphere: Statistical comparisons and scientific issues, *J. Geophys. Res.*, *107*(A12), 1468, doi:10.1029/2002JA009430.
- Richmond, A. D., and Y. Kamide (1988), Mapping electrodynamic features of the high latitude ionosphere from localized observations: Technique, *J. Geophys. Res.*, *93*, 5741–5759, doi:10.1029/JA093iA06p05741.
- Roble, R. G., and E. C. Ridley (1994), Thermosphere-Ionosphere-Mesosphere-Electro Dynamics General Circulation Model (TIME-GCM): Equinox solar cycle minimum simulations (300–500 km), *Geophys. Res. Lett.*, *21*, 417–420, doi:10.1029/93GL03391.
- Schlegel, K., H. Lühr, J. P. St. Maurice, G. Crowley, and C. Hackert (2005), Thermospheric density structures over the polar regions observed with CHAMP, *Ann. Geophys.*, *23*, 1659–1672.
- Schoendorf, J., G. Crowley, and R. G. Roble (1996), Neutral density cells in the high latitude thermosphere—2. Mechanisms, *J. Atmos. Terr. Phys.*, *58*, 1769–1781, doi:10.1016/0021-9169(95)00166-2.
- Sutton, E. K., R. S. Nerem, and J. M. Forbes (2007), Density and winds in the thermosphere deduced from accelerometer data, *J. Spacecr. Rockets*, *44*, 1210–1219, doi:10.2514/1.28641.

G. Crowley, ASTRA, 12703 Spectrum Dr., San Antonio, TX 78249, USA. (gcrowley@astraspace.net)

K. A. Drake, CIRES, University of Colorado at Boulder, Boulder, CO 80309-0216, USA.

D. J. Knipp, High Altitude Observatory, NCAR, Boulder, CO 80307-3000, USA.

J. Lei, Aerospace Engineering Sciences Department, University of Colorado at Boulder, Boulder, CO 80309, USA.

H. Lühr, Deutsches GeoForschungsZentrum, Potsdam D-14473, Germany.

E. Sutton, AFRL, Hanscom Air Force Base, MA 01731, USA.